International Atomic Energy Agency

INDC(CCP)-281/L

INDC INTERNATIONAL NUCLEAR DATA COMMITTEE

TRANSLATION OF SELECTED PAPERS PUBLISHED

IN NUCLEAR CONSTANTS, No. 3 (57)

Moscow 1984

(Original Report in Russian was distributed
as INDC(CCP)-240/G)

Translated by the IAEA

January 1988

IAEA NUCLEAR DATA SECTION, WAGRAMERSTRASSE 5, A-1400 VIENNA

TRANSLATION OF SELECTED PAPERS PUBLISHED

IN NUCLEAR CONSTANTS, No. 3 (57)

Moscow 1984

(Original Report in Russian was distributed
as INDC(CCP)-240/G)

Translated by the IAEA

January 1988

Reproduced by the IAEA in Austria
January 1988

88-00267

Table of Contents

The Spectra of Gamm-Rays from the Interaction of 3-MeV Neutrons with ^{232}Th, ^{235}U and ^{238}U Nuclei 5
M.V. Blinov, B.D. Stsiborskij, A.A. Filatenkov and B.M. Shiryaev

Measurement of the ^{237}Np and ^{235}U Fission Cross-Section Ratio by the Isotopic Dilution Method 17
A.A. Goverdovskij, A.K. Gordyushin, B.D. Kuz'minov, V.F. Mitrofanov, A.I. Sergachev, S.M. Solov'ev and P.S. Soloshenkov

Energy Dependence of the Fast-Neutron-Induced Fission Cross-Section of ^{243}Am 23
Eh. Fomushkin, G.F. Novoselov, Yu.I. Vinogradov, V.V. Gavrilov, B.K. Maslennikov, V.N. Polynov, V.M. Surin and A.M. Shvetsov

The Cross-Section of the $^{199}Hg(n,n')^{199}Hg^{m}$ Reaction for Use in Neutron Activation Measurements 29
E.I. Grigor'ev and V.P. Yaryna

Evaluation of the ^{235}U Fission Cross Section in the 14.5-14.7 MeV Neutron Energy Region 33
V.N. Dushin, A.V. Komichev, V.I. Shpakov, and S.S. Kovalenko

Analytical Representation on the Basis of the Pade Approximation of the Threshold Reaction Cross-Sections from the Dosimetry File 39
S.A. Badikov, A.I. Blokhin, E.V. Gaj, V.N. Manokhin and N.S. Rabotnov

Abstract

Translation of six papers, selected for the nuclear data interest, which were published in "Topics in Atomic Science and Technology", Series Nuclear Constants, No. 3 (57), Moscow (1984). The original report was distributed as INDC(CCP)-240/G.

THE SPECTRA OF GAMMA-RAYS FROM THE INTERACTION OF 3-MeV NEUTRONS WITH ^{232}Th, ^{235}U AND ^{238}U NUCLEI

(Original recieved 8 February 1984)

M.V. Blinov, B.D. Stsiborskij, A.A. Filatenkov and B.M. Shiryaev

ABSTRACT

Measurements were made of the gamma-ray spectra in the interaction reactions of 3-MeV neutrons with the ^{232}Th, ^{235}U and ^{238}U nuclei. There were 80 gamma transitions observed in the ^{232}Th(n,n'γ) reaction, 90 in the ^{235}U(n,n'γ) reaction and 185 in the ^{238}U(n,n'γ) reaction.

The need to study the inelastic interaction of neutrons with the structural and fissile materials of nuclear reactors arises from the practical problem of designing effective shielding and of shaping the neutron spectrum of the reactor. These studies are also used for determination of the various characteristics of nuclei and analysis of nuclear reactions: energies of excited states of nuclei, spectroscopic states and reaction cross-sections.

In the case of actinide nuclei, such studies are significantly complicated by the high density of the excited states and also by the prompt gamma-rays during the fission of nuclei. For this reason, there are not many studies dealing with the inelastic scattering of fast neutrons for actinide nuclei. A few studies have been published so far on the measurement of the discrete spectra of gamma rays accompanying fast neutron interation with ^{232}Th and ^{238}U nuclei [1-3]. There are no such publications in the case of ^{235}U. The most consistent systematization and analysis of the results for ^{232}Th and ^{238}U is to be found in Ref. [4].

The present paper gives the results of measurement of the gamma-ray spectra during the interaction of 3 MeV neutrons with ^{232}Th, ^{235}U and ^{238}U nuclei. These results, obtained in the last few years, have been published in part [5-7]. The higher neutron energy in these studies in

comparison with those of other authors imparted an additional contribution of the highly-excited states of nuclei so that it was possible to detect a larger number of gamma transitions.

Neutrons were obtained by the $^{2}H(d,n)^{3}He$ reaction in an NG-400 neutron generator, which generated 1 MHz pulses with a duration of 3 ns at FWHM. The samples to be irradiated were in the form of cylinders made of metallic ^{232}Th, ^{238}U and ^{235}U (99% enriched), and they were placed successively at a distance of 4 cm from the accelerator target at an angle of 0^{o} to the beam of accelerated deuterium ions. The ^{232}Th and ^{238}U samples had a diameter of 22 mm and a height of 27 mm, while the ^{235}U sample was 15 mm in diameter and 28 mm in height. The gamma-rays were recorded with a DGDK-40 Ge(Li) detector positioned at an angle of 125^{o} to the direction of the neutron flux incident on the sample. For reduction of the background the detector was enclosed in a circular shield consisting of lead and hydrogen-containing materials with the addition of boron. The time-of-flight technique was used with a view to further reducing the background due to the pulsed source neutrons entering the detector. For purposes of spectrum analysis we chose only events for the "time window" with a width of 20 ns centred around the prompt gamma-ray peak. The FWHM of this peak was 6-7 ns. The energy resolution of the whole system for a measurement duration of 100 h was about 4 keV at a gamma-ray energy of 1 MeV.

The background was measured both without a sample and with irradiation of a sample of oxalic acid (chemical formula $H_2C_2O_4$). For the energy and efficiency calibration of the gamma spectrometer we used a ^{226}Ra source, which was located at the place of the sample under study. The data on the gamma-ray spectrum of the ^{226}Ra decay products in equilibrium are taken from Ref. [8].

The instrument spectra of the gamma-rays from the ^{232}Th and ^{238}U samples were processed on a Minsk-22 computer by the PROSPEKT program [9], and the spectrum for ^{235}U on the ES-1033 computer by the SAMPO program [10]. As

a result of processing we obtained 80 gamma transitions for the $^{232}Th(n,n'\gamma)$ reaction (Table 1), 90 for the $^{235}U(n,n'\gamma)$ reaction (Table 2) and 185 for the $^{238}U(n,n'\gamma)$ reaction. The discrete gamma-rays due to the background of the building and the facility and to the self-radiation of the samples are not included in the tables.

Table 1.

Characteristics of gamma-transitions in the ^{232}Th $(n,n'\gamma)$ reaction

$E_\gamma(\Delta E_\gamma)$, keV	$I_\gamma(\Delta I_\gamma)$	E_i, keV	$J_i^\pi K_i$	E_f, keV	$J_f^\pi K_f$
170,9(4)	41(13)	334,0	6^+0^+	162,4	4^+0^+
222,6(6)	13(5)	1183,0	3^-3^-	960,2	5^+2^+
332,1(5)	19(4)	1105,7	3^-2^-	774,1	2^+0^+ or 3^-0^-
402,2(6)	7(2)	-	-	-	-
423,4(7)	6(2)	-	-	-	-
430,9(5)	7(2)	1143,3	4^-2^-	714,25	1^-0^-
442,7(7)	5(2)	-	-	-	-
456,2(6)	6(2)	-	-	-	-
468,6(5)	7(2)	1183,0	3^-3^-	714,25	1^-0^-
486,2(5)	8(2)	-	-	-	-
523,7(6)	6(2)	-	-	-	-
550,5(1)	55(6)	883,3	5^-0^-	334,0	6^+0^+
606,8(7)	5(2)	-	-	-	-
612,4(1)	114(9)	774,1	2^+0^+	162,4	4^+0^+
626,6(5)	8(3)	960,2	5^+2^+	334,0	6^+0^+
627,8(5)	7(3)	-	-	-	-
665,5(1)	100(7)	714,25	1^-0^-	49,4	2^+0^+
779,0(6)	9(3)	829,6	3^+2^+	162,4	4^+0^+
681,2(3)	13(2)	730,10	0^+0^+	49,4	2^+0^+
693,2(5)	11(2)	-	-	-	-
706,7(3)	14(2)	-	-	-	-
714,1(6)	16(3)	714,25	1^-0^-	0,0	0^+0^+
717,5(5)	12(3)	-	-	-	-
727,9(9)	49(10)	890,1	4^+2^+	162,4	4^+0^+
735,0(1)	62(6)	785,2	2^+2^+	49,4	2^+0^+
750,4(7)	5(2)	-	-	-	-
759,0(8)	5(2)	-	-	-	-
773,7(3)	12(3)	774,1	2^+0^+	0,0	0^+0^+
780,3(1)	63(6)	829,6	3^+2^+	49,4	2^+0^+
785,5(1)	33(4)	785,2	2^+2^+	0,0	0^+0^+
798,3(3)	21(3)	960,2	5^+2^+	162,4	4^+0^+
823,9(3)	12(2)	873,0	4^+0^+	49,4	2^+0^+
840,5(4)	7(2)	890,1	4^+2^+	49,4	2^+0^+
885,7(7)	5(2)	-	-	-	-
931,0(9)	4(2)	1094,4	2^-1^-	162,4	4^+0^+
936,1(8)	4(2)	-	-	-	-
943,4(7)	4(1)	1105,7	3^-2^-	162,4	4^+0^+
958,9(3)	10(2)	1122,8	2^+0^+	162,4	4^+0^+
981,3(2)	23(3)	1143,3	4^-2^-	162,4	4^+0^+
986,7(6)	5(2)	1148,3	4^+0^+	162,4	4^+0^+

Table 1 continued

E_γ,(ΔE_γ), keV	I_γ(ΔI_γ)	E_i, keV	$J_i^\pi K_i$	E_f, keV	$J_f^\pi K_f$
1002,5(8)	8(1)	1053,6	2^-2^-	49,4	2^+0^+
1023,6(1)	37(4)	1072,9	2^+2^+	49,4	2^+0^+
1029,5(3)	13(2)	1078,7	0^+0^+	49,4	2^+0^+
1047,0(2)	17(2)	1208,9	5^-2^-	162,4	4^+0^+
1056,3(1)	41(4)	1105,7	3^-2^-	49,4	2^+0^+
1063,4(5)	6(1)				
1072,6(2)	36(4)	1072,9	2^+2^+	0,0	0^+0^+
1077,1(2)	34(4)	1077,5	1^-1^-	0,0	0^+0^+
1133,3(2)	26(3)	1182,5	3^-3^-	49,4	2^+0^+
1166,9(3)	11(2)	-	-	-	-
1226,0(8)	8(1)	-	-	-	-
1231,4(7)	5(1)	-	-	-	-
1305,2(8)	8(1)	-	-	-	-
1324,6(5)	5(1)	-	-	-	-
1337,5(6)	5(1)	-	-	-	-
1356,8(10)	8(1)	-	-	-	-
1400,3(4)	7(1)	-	-	-	-
1486,4(7)	4(1)	-	-	-	-
1503,8(3)	11(2)	-	-	-	-
1529,5(10)	8(1)	-	-	-	-
1555,4(7)	5(1)	-	-	-	-
1561,6(9)	4(1)	-	-	-	-
1571,6(4)	9(2)	-	-	-	-
1640,2(7)	5(1)	-	-	-	-
1663,8(11)	3(1)	-	-	-	-
1680,0(12)	3(1)	-	-	-	-
1688,0(13)	8(1)	-	-	-	-
1693,6(9)	4(1)	-	-	-	-
1723,0(12)	5(1)	-	-	-	-
1832,8(10)	3(1)	-	-	-	-
1870,5(13)	3(1)	-	-	-	-
1894,1(11)	3(1)	-	-	-	-
1902,8(13)	3(1)	-	-	-	-
1941,7(7)	5(2)	-	-	-	-
1952,5(13)	4(1)	-	-	-	-
1997,6(11)	3(1)	-	-	-	-
2171,9(10)	3(1)	-	-	-	-
2232,3(11)	3(1)	-	-	-	-
2264,3(12)	3(1)	-	-	-	-
2303,9(18)	2(1)	-	-	-	-

In calculating the relative gamma-ray intensities it was assumed that the magnitude of absorption of gamma-rays in the samples was the same as in the case of a cylinder with activity distributed uniformly over volume [11]. Calculations by the Monte Carlo method [12] taking into account the experimental geometry, the space-energy distribution of neutrons of the source and its finite dimensions and with allowance for changes in the spectrum and flux density of neutrons as a result of virgin neutron elastic and inelastic

Table 2.

Characteristics of gamma-transitions in the ^{235}U (n,n'γ) reaction

$E_\gamma(\Delta E_\gamma)$, keV	$I_\gamma(\Delta I_\gamma)$	E_i, keV	$J_i^\pi K_i$	E_f, keV	$J_f^\pi K_f$
159,1(3)	270(80)	491,9	$7/2^+$	332,8	$5/2^+$
179,8(3)	154(40)	–	–	–	–
288,2(4)	34(7)	–	–	–	–
296,2(2)	64(9)	–	–	–	–
310,8(10)	22(3)	–	–	–	–
331,63(3)	67(9)	–	–	–	–
343,2(2)	51(7)	–	–	–	–
346,5(6)	20(6)	–	–	–	–
352,04(6)	115(9)	–	–	–	–
359,8(3)	48(12)	–	–	–	–
369,6(1)	58(7)	–	–	–	–
376,1(3)	45(7)	–	–	–	–
392,94(6)	24(5)	393,2	$3/2^+$	0,0	$7/2^-$
400,2(2)	39(5)	445,7	$7/2^+$	46,2	$9/2^-$
415,0(1)	34(3)	–	–	–	–
423,4(2)	23(3)	–	–	–	–
428,1(1)	47(4)	–	–	–	–
431,2(1)	51(4)	–	–	–	–
434,9(3)	19(3)	–	–	–	–
445,7(1)	22(3)	491,9	$7/2^+$	46,2	$9/2^-$
451,1(3)	26(5)	–	–	–	–
456,8(2)	51(9)	–	–	–	–
468,3(4)	14(4)	–	–	–	–
474,8(1)	54(5)	–	–	–	–
482,2(1)	93(9)	–	–	–	–
484,4(4)	32(8)	–	–	–	–
492,2(3)	26(4)	–	–	–	–
497,6(2)	26(4)	–	–	–	–
536,4(4)	19(3)	–	–	–	–
554,3(3)	18(3)	–	–	–	–
566,0(3)	35(5)	–	–	–	–
583,5(1)	63(5)	–	–	–	–
588,86(5)	94(6)	–	–	–	–
606,3(2)	28(4)	1085,1	$5/2^+$	426,7	$5/2^+$
619,2(2)	41(6)	–	–	–	–
625,2(2)	34(6)	671,0	$7/2^-$	46,2	$9/2^-$
681,5(8)	44(7)	–	–	–	–
646,9(2)	19(4)	659,0	–	18,0	$3/2^+$
654,6(8)	21(4)	701,0	–	46,2	$9/2^-$
658,7(2)	26(4)	659,0	–	0,0	$7/2^-$
667,0(8)	22(4)	–	–	–	–
682,3(4)	12(2)	–	–	–	–
706,88(7)	100(7)	–	–	–	–
718,2(5)	10(3)	848,7	$3/2^+$	129,8	$5/2^+$
729,6(2)	31(5)	–	–	–	–
761,1(3)	14(2)	760,9	$1/2^+$	0,0	$7/2^-$
768,7(1)	40(5)	–	–	–	–
775,7(1)	31(4)	1202,6	$3/2^-$	426,7	$5/2^+$
781,8(5)	6(2)	–	–	–	–
798,8(3)	18(3)	–	–	–	–
802,4(2)	33(5)	–	–	–	–
808,1(3)	15(3)	–	–	–	–
813,6(3)	21(4)	–	–	–	–
815,12(7)	59(8)	–	–	–	–

Table 2 Continued

$E_\gamma(\Delta E_\gamma)$, keV	$I_\gamma(\Delta I_\gamma)$	E_i, keV	$J_i^\pi K_i$	E_f, keV	$J_f^\pi K_f$
831,8(5)	12(3)	1057,3	$7/2^+$	225,4	$9/2^+$
837,1(1)	76(9)	–	–	–	–
863,1(3)	13(4)	1035,1	$5/2^+$	171,3	$7/2^+$
868,7(2)	19(4)	–	–	–	–
882,2(4)	12(4)	–	–	–	–
886,6(4)	13(4)	1057,3	$7/2^+$	171,3	$7/2^+$
908,6(3)	12(3)	–	–	–	–
913,3(1)	85(5)	–	–	–	–
920,4(4)	13(3)	–	–	–	–
933,7(4)	7(2)	–	–	–	–
940,9(2)	13(2)	–	–	–	–
953,5(2)	30(4)	–	–	–	–
977,6(3)	19(5)	–	–	–	–
987,4(4)	19(5)	1116,2	$5/2^+$	129,3	$5/2^+$
998,1(3)	17(4)	–	–	–	–
1010,1(4)	14(3)	–	–	–	–
1014,6(1)	38(6)	–	–	–	–
1022,4(8)	14(8)	–	–	–	–
1031,9(9)	8(3)	–	–	–	–
1089,2(2)	16(3)	–	–	–	–
1133,9(1)	85(5)	–	–	–	–
1160,3(6)	11(1)	–	–	–	–
1181,8(8)	21(2)	–	–	–	–
1220,0(2)	42(5)	–	–	–	–
1228,6(2)	45(5)	–	–	–	–
1279,8(2)	24(4)	–	–	–	–
1294,4(4)	19(4)	–	–	–	–
1307,8(2)	94(6)	1821,2	$5/2^+$	13,0	$9/2^+$
1311,9(5)	13(4)	–	–	–	–
1362,5(3)	21(2)	–	–	–	–
1426,8(7)	8(2)	1438,6	$5/2^+$	13,0	$9/2^+$
1437,1(3)	13(3)	–	–	–	–
1441,3(3)	10(3)	–	–	–	–
1454,1(4)	14(3)	–	–	–	–
1509,1(3)	12(3)	–	–	–	–

scattering in samples, fission reactions and radiative capture gave coinciding values of the attenuation coefficients. Apart from these calculations, we also made control measurements in which the cylindrical ^{232}Th and ^{238}U samples were replaced by plates of the same materials so arranged that the normal to the plate surface bisected the angle between the directions to the source and to the detector. The results of the control measurements agreed within errors with those of the main experiment.

Tables 1-3 give the energies $E\gamma$ and relative intensities $I\gamma$ of the detected gamma-transitions and the errors of the values given (in brackets) expressed in units of the last digit of the corresponding value. The error of

determination of the gamma-transition energy is the sum of the errors of determination of the position of the gamma-peak in the spectrum (0.03-1.2 keV) and energy calibration of the gamma spectrometer (about 0.1 keV). In determining the errors of the gamma-transition intensities we took into account the error in calculation of the gamma-peak area (1-30%), the error in determination of the relative efficiency of the Ge(Li) detector (1.5-8%) and the error in calculation of the attenuation coefficient of the gamma-ray flux from the sample (4-15%). The tables also give the energies E, spins J, projections of the total angular moment on the axis of symmetry of the nucleus

Table 3

Characteristics of gamma-transitions in the ^{238}U (n,n'γ) reaction

E_γ(ΔE_γ), keV	I_γ(ΔI_γ)	E_i, keV	$J_i^\pi K_i$	E_f, keV	$J_f^\pi K_f$
141,2(2)	49(40)	-	-	-	-
159,5(3)	70(22)	307,2	6^+0^+	148,4	4^+0^+
163,5(10)	21(12)	-	-	-	-
193,4(10)	10(6)	—	-	-	-
198,6(3)	14(7)	1128,7	2^-2^-	930,8	1^-1^-
203,4(10)	6(6)	-	-	-	-
208,3(10)	17(5)	—	-	-	-
212,3(4)	19(6)	518,3	8^+0^+	307,2	6^+0^+
218,0(3)	15(5)	950,0	2^-1^-	731,9	3^-0^-
223,4(4)	17(4)	-	-	-	-
248,6(7)	9(4)	-	-	-	-
251,3(10)	4(4)	930,8	1^-1^-	680,1	1^-0^-
260,0(13)	4(3)	-	-	-	-
270,1(4)	11(4)	950,0	2^-1^-	680,1	1^-0^-
274,0(10)	7(3)	-	-	-	-
282,2(6)	7(3)	-	-	-	-
287,9(4)	11(3)	-	-	-	-
296,6(4)	9(3)	/1245,9/	-	950,0	2^-1^-
300,6(10)	4(3)	-	-	-	-
325,9(2)	18(3)	1057,5	-	731,9	3^-0^-
331,6(2)	17(3)	/1368,1/	-	1037,3	2^+0^+
352,3(1)	26(2)	-	-	-	—
357,7(4)	7(2)	1037,3	2^+0^+	680,1	1^-0^-
369,5(2)	13(2)	/1368,1/	-	997,5	3^-1^-
376,7(2)	18(2)	-	-	-	-
396,3(2)	18(2)	1128,7	2^-2^-	731,9	3^-0^-
401,6(3)	10(2)	-	-	-	-
405,8(10)	4(2)	/1355,1/	-	950,0	2^-1^-
423,8(3)	10(2)	/1355,1/	-	930,8	1^-1^-
428,5(10)	5(2)	-	-	-	-
432,5(3)	8(2)	—	-	-	-
436,8(3)	10(2)	-	-	-	-

Table 3 Continued

$E_\gamma(\Delta E_\gamma)$ keV	$I_\gamma(\Delta I_\gamma)$	E_i, keV	$J_i^\pi K_i$	E_f, keV	$J_f^\pi K_f$
443,8(10)	5(2)				
448,4(9)	27(3)	965,9	7^-0^-	517,8	8^+0^+
		1128,7	2^-2^-	680,1	1^-0^-
457,7(1)	18(2)	–	–	–	–
482,9(3)	7(2)	–	–	–	–
486,8(10)	6(2)	–	–	–	–
490,3(2)	11(2)	1222,9	2^+	731,9	3^-0^-
497,3(3)	9(2)	–	–	–	–
501,0(10)	7(2)	–	–	–	–
519,44(8)	25(2)	827,2	5^-0^-	307,2	6^+0^+
536,8(4)	5(2)	–	–	–	–
547,0(3)	8(2)	–	–	–	–
552,5(10)	5(2)	–	–	–	–
555,3(5)	5(2)	–	–	–	–
566,1(3)	9(2)	–	–	–	–
583,55(3)	82(3)	731,9	3^-0^-	148,4	4^+0^+
589,1(2)	9(2)	–	–	–	–
606,6(2)	25(3)	–	–	–	–
620,4(3)	7(2)	–	–	–	–
625,2(2)	11(2)	–	–	–	–
629,6(10)	8(2)	–	–	–	–
635,18(3)	100(3)	680,1	1^-0^-	44,9	2^+0^+
641,3(4)	5(2)	–	–	–	–
647,7(4)	6(2)	–	–	–	–
651,8(10)	5(2)	–	–	–	–
655,0(10)	5(2)	–	–	–	–
659,1(2)	14(2)	965,9	7^-0^-	307,2	6^+0^+
679,5(3)	107(5)	827,2	5^-0^-	148,4	4^+0^+
680,1(3)		680,1	1^-0^-	0,0	0^+0^+
686,99(3)	91(5)	731,9	3^-0^-	44,9	2^+0^+
706,6(2)	16(2)	–	–	–	–
711,0(10)	2(2)	–	–	–	–
738,5(10)	3(2)	–	–	–	–
749,3(2)	11(2)	–	–	–	–
758,8(4)	4(1)	–	–	–	–
768,3(2)	11(1)	–	–	–	–
774,7(4)	5(1)	–	–	–	–
783,0(10)	2(1)	–	–	–	–
786,0(10)	1(1)	–	–	–	–
798,9(2)	11(1)	–	–	–	–
808,4(1)	14(2)	–	–	–	–
814,8(2)	11(2)	–	–	–	–
818,1(2)	17(2)	966,3	2^+0^+	148,4	4^+0^+
828,3(6)	3(1)	–	–	–	–
836,7(2)	9(1)	–	–	–	–
849,7(2)	28(3)	997,5	3^-1^-	148,4	4^+0^+
855,5(3)	7(1)	–	–	–	–
863,5(6)	3(1)	–	–	–	–
880,8(2)	11(1)	927,0	0^+0^+	44,9	2^+0^+

Table 3 Continued

$E_\gamma(\Delta E_\gamma)$, keV	$I_\gamma(\Delta I_\gamma)$	E_i, keV	$J_i^\pi K_i$	E_f, keV	$J_f^\pi K_f$
885,8(3)	65(4)	930,8	1^-1^-	44,9	2^+0^+
905,6(6)	30(2)	950,0	2^-1^-	44,9	2^+0^+
911,4(5)	29(2)	1060,3	2^+2^+	148,4	4^+0^+
922,3(2)	8(1)	966,3	2^+0^+	44,9	2^+0^+
932,7(3)	8(1)	–	–	–	–
952,70(7)	30(2)	997,5	3^-1^-	44,9	2^+0^+
957,33(6)	32(2)	1105,6	3^+2^+	148,4	4^+0^+
962,0(10)	4(1)	–	–	–	–
967,3(2)	11(2)	966,3	2^+0^+	0,0	0^+0^+
978,5(3)	7(1)	–	–	–	–
993,0(10)	3(1)	1037,3	2^+0^+	44,9	2^+0^+
1015,06(2)	115(7)	1060,3	2^+2^+	44,9	2^+0^+
1019,61(8)	28(2)	1167,7	4^+2^+	148,4	4^+0^+
1033,2(5)	4(1)	–	–	–	–
1037,4(2)	8(1)	1037,3	2^+0^+	0,0	0^+0^+
1043,0(10)	1(1)	–	–	–	–
1055,9(4)	4(1)	–	–	–	–
1060,98(8)	67(4)	1105,6 1060,3	3^+2^+ 2^+2^+	44,9 0,0	2^+0^+ 0^+0^+
1074,4(2)	7(1)	–	–	–	–
1084,13(7)	26(2)	1128,7	2^-2^-	44,9	2^+0^+
1090,9(2)	12(1)	–	–	–	–
1112,7(3)	7(1)	–	–	–	–
1123,1(2)	11(1)	1167,7	4^+2^+	44,9	2^+0^+
1132,2(3)	6(1)	–	–	–	–
1138,0(10)	3(1)	–	–	–	–
1153,0(10)	2(1)	–	–	–	–
1160,4(2)	10(1)	–	–	–	–
1173,4(7)	3(1)	–	–	–	–
1179,4(2)	15(2)	–	–	–	–
1200,6(4)	4(1)	–	–	–	–
1209,3(3)	6(1)	–	–	–	–
1215,9(2)	11(1)	–	–	–	–
1223,2(2)	10(1)	1222,9	2^+	0,0	0^+0^+
1233,8(3)	8(1)	–	–	–	–
1262,0(10)	2(1)	–	–	–	–
1265,6(10)	3(1)	–	–	–	–
1273,0(10)	3(1)	–	–	–	–
1278,8(2)	10(1)	1278,9	–	0,0	0^+0^+
1286,0(10)	3(1)	–	–	–	–
1296,0(10)	3(1)	–	–	–	–
1306,1(4)	5(1)	–	–	–	–
1310,5(4)	5(1)	[1855,1]	–	44,9	2^+0^+
1336,2(3)	5(1)	[2168,5]		827,2	5^-0^-
1354,5(10)	3(1)	[1855,1]		0,0	0^+0^+
1361,5(10)	5(1)	—			
1368,3(2)	18(1)	[1368,1]		0,0	0^+0^+
1376,8(9)	2(1)				
1381,8(5)	4(1)				

Table 3 Continued

$E_\gamma(\Delta E_\gamma)$, keV	$I_\gamma(\Delta I_\gamma)$	E_i, keV	$J_i^\pi K_i$	E_f keV	$J_f^\pi K_f$
1410,7(2)	8(1)	–	–	–	–
1417,5(4)	5(1)	–	–	–	–
1428,5(10)	2(1)	–	–	–	–
1431,3(10)	4(1)	[2163,5]	–	731,9	3^-0^-
1437,1(2)	19(2)	–	–	–	–
1441,4(10)	3(1)	–	–	–	–
1446,2(3)	8(1)	–	–	–	–
1454,0(10)	3(1)	–	–	–	–
1458,0(10)	6(1)	–	–	–	–
1464,0(10)	4(1)	–	–	–	–
1470,0(10)	7(1)	–	–	–	–
1485,0(10)	2(1)	–	–	–	–
1489,0(10)	2(1)	–	–	–	–
1495,0(10)	4(1)	–	–	–	–
1507,1(3)	8(1)	–	–	–	–
1511,0(10)	3(1)	–	–	–	–
1523,7(3)	5(1)	–	–	–	–
1531,6(10)	2(1)	–	–	–	–
1545,9(12)	2(1)	–	–	–	–
1550,0(4)	6(1)	–	–	–	–
1560,2(10)	2(1)	–	–	–	–
1563,5(10)	2(1)	–	–	–	–
1584,9(3)	7(1)	–	–	–	–
1598,2(4)	5(1)	–	–	–	–
1609,0(10)	2(1)	–	–	–	–
1614,8(10)	2(1)	–	–	–	–
1627,3(6)	3(1)	–	–	–	–
1705,0(12)	3(2)	–	–	–	–
1716,7(6)	4(1)	–	–	–	–
1737,4(4)	5(1)	–	–	–	–
1750,2(3)	5(1)	–	–	–	–
1759,6(3)	6(1)	–	–	–	–
1768,5(10)	2(1)	–	–	–	–
1778,1(6)	4(1)	–	–	–	–
1782,0(10)	4(1)	–	–	–	–
1801,9(4)	6(1)	–	–	–	–
1807,0(10)	3(1)	–	–	–	–
1814,1(10)	3(1)	–	–	–	–
1826,9(4)	5(1)	–	–	–	–
1833,0(10)	3(1)	–	–	–	–
1844,6(5)	4(1)	–	–	–	–
1856,6(4)	6(1)	[2163,5]	–	307,2	6^+0^+
1862,5(10)	3(1)	–	–	–	–
1874,0(8)	2(1)	–	–	–	–
1882,0(10)	3(1)	–	–	–	–
1888,3(5)	4(1)	–	–	–	–
1905,1(4)	5(1)	–	–	–	–
1911,0(10)	2(1)	–	–	–	–
1923,0(10)	2(1)	–	–	–	–

Table 3 Continued

$E_\gamma(\Delta E_\gamma)$, keV	$I_\gamma(\Delta I_\gamma)$	E_i, keV	$J_i^\pi K_i$	E_f, keV	$J_f^\pi K_f$
1930,0(10)	2(1)	–	–	–	–
1994,0(3)	6(1)	–	–	–	–
2007,0(10)	1(1)	–	–	–	–
2014,8(4)	5(1)	/2163,5/		148,4	4^+0^+
2030,0(10)	–	–	–	–	–
2034,8(5)	5(1)	–	–	–	–
2052,0(6)	3(1)	–	–	–	–
2791,1(6)	2,5(8)	–	–	–	–

K and the parities π of the initial i and final f states of nuclei, to the transition between which the given gamma radiation can be attributed in accordance with the level schemes of ^{232}Th and ^{238}U [2-4, 13].

Data on excited states with E* > 1.2 MeV are clearly inadequate. Attempts to supplement the level schemes of ^{232}Th and ^{238}U by the method of energy coincidences of gamma transitions using the results obtained met with difficulties. These were caused both by the large probability of random coincidences of gamma-transition energies due to the considerable level density and insufficient accuracy of determination of the weak-gamma-ray energy and by the possibility of the presence of fission-fragment gamma rays. Identification of the latter is not a trivial problem since the gamma-ray spectra during the fission even of nuclei which are close in mass may differ substantially [14]. In Table 3 we have therefore given several new recommended excitation levels for the ^{238}U nucleus (the energies of these levels are indicated in square brackets), for which the evaluated probability of random coincidence is 0.05-0.1.

REFERENCES

[1] POENITZ, W.P., Nucl. Data for Reactors. Helsinki (1970) 2, p. 3.

[2] McMURRAY, W.R., VAN HEERDEN, I.J., Z. Phys. (1972) 253, p. 289.

[3] DEMIDOV, A.M., GOVOR, L.I., CHEREPANTSEV, Yu.K., et al., Atlas of the Gamma-Ray Spectra of Reactor Fast Neutron Inelastic Scattering, Atomizdat, Moscow (1978) 311-316 (in Russian).

[4] CHAN, D.W.S., EGAN, J.J., MITTLER, A., SHELDON, E., Phys. Rev. C., (1982) 26, N 3, p. 841-888.

[5] KOZULIN, Eh.M., TUTIN, G.A., FILATENKOV, A.A., Neutron Physics (Proceedings of the Fifth All-Union Conference on Neutron Physics, Kiev, 15-19 September 1980) part 2, TsNIIatominform, Moscow, (1980) 25-29 (in Russian).

[6] BLINOV, M.V., et al., Abstracts of Papers Presented at the 33rd Meeting on Nuclear Spectroscopy and the Structure of the Atomic Nucleus, Moscow (1983) 313-314 (in Russian).

[7] BLINOV, M.V., STSIBORSKIJ, B.D., FILATENKOV, A.A., SHIRYAEV, B.M., Zentralist. Kernforsch. Rossendorf Dresden (Ber.) Proc.11 Intern.Symp. Interact. Fast Neutron Nuclei. 1982, N 476, p. 116-119.

[8] ZOBOL, V. et al., Nucl. Instrum. and Methods (1977) N 141, p. 329.

[9] KABINA, L.P., KONDUROV, I.A., FEDOROVA, Eh.I, Report LIYaF-123, Leningrad (1974) (in Russian).

[10] ROUTTI, J.T., PRUSSIAN, S.G., Nucl. Instrum. and Methods (1969) 72, p. 125-142.

[11] GORSHKOV, G.V., Gamma Radiation of Radioactive Substances and Components of Radiation Shielding, Moscow-Leningrad (1959) 64 (in Russian).

[12] DUSHIN, V.N., FILATENKOV, A.A., See [5], part 4, pp. 242-244 (in Russian).

[13] ELLIS, Y.A., Nucl. Data Sheets (1977) 21, N 1, p. 549.

[14] TELEREV, Eh.N., VAL'SKIJ, G.V., PETROV, G.A., PLEVA, Yu.S., Neutron Physics (Proceedings of the Third All-Union Conference on Neutron Physics, Kiev, 9-13 June 1975) part 6, TsNIIatominform (1976) 121 (in Russian).

MEASUREMENT OF THE ^{237}Np and ^{235}U FISSION CROSS-SECTION RATIO BY THE ISOTOPIC DILUTION METHOD

(original received 1 February 1984)

A.A. Goverdovskij, A.K. Gordyushin, B.D. Kuz'minov,
V.F. Mitrofanov, A.I. Sergachev, S.M. Solov'ev
and P.S. Soloshenkov

ABSTRACT

The ^{237}Np and ^{235}U fission cross-section ratio has been measured with a total error of 2.5% for 7.3 and 16.4 MeV neutron energies. The $T(p,n)^3He$, $T(d,n)^4He$ and $D(d,n)^3He$ reactions were used as the neutron source.

The results of measurement by different authors of the fission cross-section of ^{237}Np (σ_f^7) for neutrons above 6 MeV vary considerably both in absolute value and in energy dependence [1]. Of the possible reasons for these discrepancies the most important are that the different components of the neutron background are taken into account and that the absolute value of the energy dependence of the fission cross-section is obtained. While the first reason is determined by the individual characteristics of each experiment, the problem of obtaining the absolute value is a general one. Since most of the data on σ_f^7 were obtained by the relative method, we shall discuss below the problems associated with the ^{237}Np and ^{235}U fission cross-section ratio, which can be represented in the form

$$\sigma_f^7/\sigma_f^5 = n_7/n_5 N_{nu}^5/N_{nu}^7 K_\varepsilon \prod_j K_j,$$

where $n_{7,5}$ denotes the counting rates of fission events, $N_{nu}^{5,7}$ is the number of nuclei in the targets, K_ε the ratio of recording efficiencies and K_j correction factors.

The ratio of the number of nuclei in the samples was determined in Ref. [2] by the method of comparison of alpha activities in a fixed geometry.

The ^{235}U nuclei have a much longer lifetime than the ^{237}Np nuclei, while the ^{234}U background is usually considerable and therefore the counting error for ^{235}U alpha-particles in the target is large. Moreover, the use of large-diameter targets makes it complicated to take into account the effects associated with the shape of the active spot and with target inhomogeneity; therefore, to obtain the absolute value of the energy dependence of the ^{237}Np and ^{235}U fission cross-section ratio it is advisable to use the isotopic dilution method or its modification - the "threshold cross-section" method [1]. In this case, the ratio $\sigma_f^7/\sigma_f^5 = \eta(R/R_{th}-1)$, where η is the relative content of ^{235}U nuclei in the ^{237}Np target, R/R_{th} the ratio of ^{237}Np and ^{235}U fission fragment count rates for fast and thermal neutrons, respectively.

Since the ^{237}Np fission cross-section has an appreciable value even at neutron energies of a few kiloelectron-volts (about 0.001), the "threshold cross-section" method [1] has to be used for targets with a high content of ^{235}U nuclei and this reduces the relative accuracy of the σ_f^7/σ_f^5 ratio. In the present study we endeavoured to measure this ratio by the istopic dilution method using electrostatic accelerators.

Fissile samples were prepared by the application of uranium and neptunium oxide solutions onto thin (30 μm) aluminium backing, followed by annealing. The inhomogeneity of target thickness (10%) was determined with a miniature semiconductor alpha-counter. The homogeneity of the uranium-neptunium mixture was checked from the shift of the fission-fragment amplitude spectra measured at a different orientation of the layer in relation to the neutron flux. The corresponding average geometrical factors were calculated by the Monte Carlo method. The target was irradiated successively in thermal and fast neutron fluxes.

The value of η was determined from the chemical analysis data and checked by alpha-spectrometry. The accuracy attained for this value was 1%. The mixtures were prepared from materials with 99.9% isotopic purity. The

Table 1. Composition and density of the targets measured

Target No.	Composition, %		Density, μg/cm²
	^{235}U	^{237}Np	
1	3.46	96.54	300
2	4.40	95.60	300
3	6.50	93.50	300
4	I8.26	8I.74	I06
5	24.65	75.35	I00
6	34.75	65.25	98
7	99.992	-	258
8	-	99.05	460
9	99.992	-	4I0

Note: Target No. 8 contained 0.52 and 0.43% ^{241}Am and ^{239}Pu, respectively.

target characteristics are given in Table 1. The isotopic weighing of the samples (determination of R_{th}) was performed in a flux of neutrons from the $T(p,n)^3He$ reaction moderated by a 20-cm thick polyethylene layer. The cadmium ratio was about 80. The fission fragment detector was a double ionization chamber filled with xenon to a pressure of $1.8 \cdot 10^5$ Pa. The recording efficiency for ^{237}Np and ^{235}U fission fragments was 91 and 98%, respectively. The ^{237}Np and ^{235}U fission cross-section ratio was measured for 7.34 and 16.4 MeV neutron energies. The neutron source was the reactions $D(d,n)^3He$ and $T(d,n)^4He$ in gaseous deuterium and solid tritium-titanium targets.

The procedure for determination of the absolute values of the σ_f^7/σ_f^5 ratio consisted of successive irradiation of assemblies of seven targets in fast and thermal neutron fluxes. Then targets Nos 8 and 9 were irradiated by fast neutrons in order to determine the effective ratio of the numbers of fissile nuclei in them (K_{eff}) by normalizing to the σ_f^7/σ_f^5 values obtained on the first seven targets.

The σ_f^7/σ_f^5 ratio for a neutron energy of 7.34 MeV was measured in the pulsed beam of an EhGP-10 M tandem generator [3]. Targets Nos 1 and 7 were

used. The selection of the energy point was determined by the low neutron background of the associated deuteron reactions and of the experimental hall. The measurement and correction procedure is similar to that described in Ref. [4].

16.4-MeV neutrons from the $T(p,n)^4He$ reaction were obtained in the continuous beam of a cascade generator. The background of the associated (d,n) reactions was determined from the increase in the relative count rates of fission fragments in "pure" and "mixed" layers, while the background of the experimental hall was determined by varying those rates between the tritium target and the fissile samples. In the E_n = 16 MeV region a fairly wide plateau was observed in the σ_f^7/σ_f^5 ratio; hence the corrections for the background of neutrons scattered on the structural materials of the target holder and the ionization chamber are small. The corrections associated with the process of passage of fragments in the layers were determined in the same way as in Ref. [5] and amounted to 0.2-0.5%. The background of secondary particles from the (n,p) and (n,α) reactions in the detector material was measured with the help of standard samples - aluminium foils without an active layer.

Table 2. Results of measurement of σ_f^7/σ_f^5 and K_{eff}

Target No.	σ_f^7/σ_f^5 for 16.4 MeV	K_{eff} for 16.4 MeV
I	I.056	I.354
2	I.044	I.339
3	I.062	I.36I
4	I.070	I.372
5	I.048	I.344
6	I.038	I.33I

Note: For target No. 1 the σ_f^7/σ_f^5 ratio and the coefficient K_{eff} for 7.34 MeV are 1,232 and 1.366, respectively.

Table 2 gives the results of measurement of the σ_f^7/σ_f^5 ratios and K_{eff}. The total measurement error was determined by several components:

- The statistical counting error of uranium and neptunium fission fragments for thermal and fast neutrons (0.3-1.0%), the error of the recording efficiency ratio (up to 1.2%) and the error of the corrections made (0.2%);
- The error of determination of the isotopic composition (1%).

The total error (about 2.5%) was calculated with allowance for the correlation of partial errors in the same manner as in Ref. [6].

Multiplying K_{eff} averaged over the set of data (see Table 2) by the corresponding non-normalized values of the ^{237}Np and ^{235}U fission cross-section ratio, we finally obtain σ_f^7/σ_f^5 equal to 1.246 ± 0.030 for 7.34 MeV and 1.049 ± 0.024 for 16.4 MeV.

The studies show that the isotope dilution method can be used for measurements of the ^{237}Np and ^{235}U fission cross-section ratio.

REFERENCES

[1] BEHRENS, J.W., BROWN, J.C., WALDEN, J.C., Measurement of the neutron-induced fission cross-section of Neptunium-237 relative to Uranium-235 from 20 keV to 30 MeV. - Nucl. Sci. and Engng. 80 (1982) 393-400.

[2] MEADOWS, J.W., The ^{237}Np to ^{235}U Fission Cross-Section Ratio: INDC(USA)-91/L., May 1983, 9-10.

[3] GOVERDOVSKIJ, A.A., GORDYUSHIN, A.K., KUZ'MINOV, B.D. et al., "Measurement of the ^{238}U and ^{235}U fission cross-section ratios in the 5.4-10.4 MeV neutron energy region", At. Ehnerg. 56 (1984) 17 (in Russian).

[4] GOVERDOVSKIJ, A.A., GORDYUSHIN, A.K., KUZ'MINOV, B.D. et al., "Measurement of the fission cross-sections of heavy nuclei by the pulse synchronization method" in: Neutron Physics (Proceedings of the Sixth

All-Union Conference On Neutron Physics, Kiev, 2-6 October 1983) 4, TSNIIatominform (1984) (in Russian).

[5] CARLSON, G.W., The effect of fragment anisotropy on fission chamber efficiency. - Nucl. Instrum. and Methods, 119 N 2, 3 (1974) 97-100.

[6] KON'SHIN, V.A., SUKHOVITSKIJ, E.Sh., ZHARKOV, V.F., Determination of errors of evaluated data with allowance for correlations and the evaluation of $\sigma_f(^{235}U)$, $\alpha(^{235}U)$, $\alpha(^{239}Pu)$ and $\sigma_f(^{239}Pu)$ for BOYaD-3. Report, A.V. Lykov Institute of Heat and Mass Exchange, Minsk (1978) (in Russian).

ENERGY DEPENDENCE OF THE FAST-NEUTRON-INDUCED FISSION CROSS-SECTION OF ^{243}Am

(Original received 19 April 1984)

Eh. Fomushkin, G.F. Novoselov, Yu.I. Vinogradov,
V.V. Gavrilov, B.K. Maslennikov, V.N. Polynov,
V.M. Surin and A.M. Shvetsov

ABSTRACT

The behaviour of the energy dependence of the ^{243}Am fission cross-section was measured by the time-of-flight technique using an underground nuclear explosion as the pulsed neutron source. The cross-section was normalized on the basis of the results of measurement of the ^{243}Am effective fission cross-section for neutrons from a metallic uranium assembly. In the $0.3 \leq E_n \leq 4.0$ MeV neutron energy region the cross-sections were approximated by a Hill-Wheeler three parameter curve of penetration through a parabolic barrier. For $E_n \sim 14.8$ MeV the ^{243}Am fission cross-section was measured with a low-voltage accelerator tube. The errors of the data obtained are analysed. The measurement results are compared with data published earlier.

Despite the relative accessibility of the ^{243}Am isotope and its comparatively long half-life (7380 years), the cross-section of the ^{243}Am(n,f) reaction has so far not been studied sufficiently well. Individual measurements show considerable scatter. This is apparently due to the fact that ^{243}Am samples obtained during the irradiation of lighter nuclides in high-flux reactors contain an appreciable quantity of ^{242}Cm formed during ^{242}Am^{m} decay. Spontaneous fission of ^{242}Cm nuclei generates a non-removable background, which makes it difficult to perform accurate measurements of the ^{243}Am fission cross-section using laboratory neutron sources with a relatively low flux at the measurement positions.

All the earlier results of measurement and evaluation of the energy dependence of the ^{243}Am fission cross-section [1-5] show that the relative dependence $\sigma_f(E_n)$ in the $0.3 \leq E_n \leq 5$ MeV region can be approximated by a curve of penetration through a parabolic barrier.

$$E_{nup} = E_{thr} \qquad (1)$$

The values of threshold energy E_{thr} and barrier curvature parameter $\hbar\omega_f$ obtained in the different measurements are in quite good agreement. However, the value of the plateau cross-section σ_{f_o} differs significantly in the measurements of individual experimental groups: approximately from 1.3 b in the evaluation of Ref. [4] to 1.7 b in the measurement of Ref. [5].

We used ^{243}Am samples obtained as a result of enrichment on an electromagnetic mass-spectrometer. Immediately after separation the samples had the following isotopic composition, at.%: ^{243}Am 100; ^{242}Am^{m} ($2.60 \pm \begin{smallmatrix}0.45\\0.90\end{smallmatrix} \times 10^{-2}$; ^{241}Am ($1.81 \pm \begin{smallmatrix}0.30\\0.60\end{smallmatrix}$) $\times 10^{-2}$; ^{240}Pu 6.6×10^{-2}; ^{244}Pu 5.5×10^{-2}.

"Weighing" of the ^{243}Am layers was performed with a semiconductor alpha-spectrometer under the conditions of a "good" geometry. The energy scale of the alpha-spectrometer was graduated with the help of standard spectrometric alpha-sources of the OSAI type (set No. 536 was made in October 1980). The number of ^{243}Am nuclei in the layer was determined from the total area of peaks with energies of 5275 keV (87.5%), 5233 keV (11%) etc. due to the ^{243}Am alpha-decay. The recording efficiency of alpha particles in the spectrometer was determined with the help of a calibrated ^{238}Pu layer also from set No. 536 of the OSAI-type alpha-sources. The half-life of ^{243}Am was taken as 7380 ± 40 years [6].

The number of ^{243}Am nuclei in each layer was determined with a total error of 2.2% ($p = 0.68$); the systematic error of this value, which is 1.37%, is mainly the sum of the error of the ^{243}Am half-life (0.54%) and the certificate error of the activity value of the ^{238}Pu reference layer

(about 1%, p = 0.68). For all neutron sources the ^{243}Am fission cross-section was measured relatively, ^{235}U layers being used as reference. The ^{235}U fission cross-section was taken from the evaluation results given in Ref. [7], and the correction for the content of ^{238}U nuclei in the reference layers was made on the basis of the mass-analysis and evaluation results [8].

The energy dependence of the ^{243}Am fission cross-section for neutrons in the 0.3–0.4 MeV region was measured by the time-of-flight technique, a nuclear explosion being used as the pulsed neutron source. The measurement procedure is described in Refs [9, 10]. The time-of-flight scanning was performed with an electromechanical device. The fission fragments of the ^{243}Am and ^{235}U nuclei – the latter used as reference – were recorded with a polymer film, which was displaced rapidly in relation to the fissile isotope layers at the instant of the neutron pulse. Slit collimators, located between each layer and the film, formed narrow beams of fission fragments. The time resolution in this case was determined by the collimator slit width $\Delta\kappa$, the rate of displacement of the film v and flight length L:

$$\Delta t/L \approx \Delta\text{æ}/vL . \qquad (2)$$

In the measurement of the ^{243}Am fission cross-section the time resolution was 5.9 ns/m (FWHM). After chemical processing the films were scanned visually with an optical microscope. The energy dependence of the neutron-induced fission cross-section of ^{243}Am was constructed on the basis of the distribution of the ^{243}Am and ^{235}U fission-fragment tracks over the film length. In the 0.3-4.0 MeV neutron energy region this dependence was approximated by the three-parameter curve of penetration through a parabolic barrier (1).

For the threshold energy and the barrier curvature parameter the values obtained were (0.90 ± 0.01) and (0.73 ± 0.02) MeV, respectively. The third parameter – the plateau cross-section value – was determined from the results of measurement of the ^{243}Am fission cross-section for neutrons of the metallic uranium assembly. In these measurements the ^{243}Am layer and

the dielectric (glass) fission-fragment detector were rigidly fixed coaxially in a so-called integral chamber. The diameters of the fissile substance layer and the detector, together with the distance between the planes of the layer and the detector, were measured with an error not greater than 0.2%. In this geometry the probability of a fragment entering the detector can be calculated with an accuracy of about 0.3% [11]. Owing to the possible inhomogeneity of distribution of ^{243}Am atoms over the layer surface, the error of the fragment recording probability was increased approximately to 1%. In the uranium assembly measurements the reference used was a calibrated layer of ^{235}U (with ^{238}U and ^{234}U impurities) from the set of detectors with fissile isotopes (neutron fissile set) No. 005 made at the All-Union Scientific Research Institute for Physicotechnical and Radiotechnical Measurements in 1980. During irradiation the chamber with the ^{243}Am and the container with the ^{235}U layer were placed in the inner cavity of the assembly, where the spatial anisotropy of the neutron flux was practically insignificant. After chemical processing the number of fission-fragment tracks on each detector was determined visually with a microscope.

Processing the data, we obtained the ratio of the ^{243}Am and ^{235}U effective fission cross-sections for the uranium assembly neutrons: $\bar{\sigma}_f{}^{243}_{Am}/\bar{\sigma}_f{}^{235}_{U} = 0.490 \pm 0.014$. The effective fission cross-section of ^{235}U with allowance for the impurity isotopes was calculated by averaging the recommended data [7, 8] over the neutron spectrum of the uranium assembly. The value of $\bar{\sigma}_f{}^{235}_{U} = (1.275 \pm 0.036)$ b was obtained per ^{235}U nucleus. Thus, the effective fission cross-section of ^{243}Am for the uranium assembly neutrons is $\bar{\sigma}_f{}^{243}_{Am} = (0.625 \pm 0.025)$ b. We have given the total error (4.0%), the components of which were indicated above.

As has been noted already, the energy dependence of the ^{243}Am fission cross-section for neutrons in the $0.3 \leq E_n \leq 4$ MeV region can be approximated quite satisfactorily by a curve of penetration through a parabolic barrier. On the basis of the values obtained for $\bar{\sigma}_f{}^{243}_{Am}$, E_{thr}, $\hbar\omega_f$ and the uranium

assembly neutron spectrum we calculated the value of the plateau cross-section as (1.411 ± 0.067) b, which is in good agreement with the results of Refs [1, 3, 4] but is appreciably lower than $\sigma_{f_c} \approx 1.71$ b obtained in Ref. [5].

The ^{243}Am fission cross-section for quasi-monochromatic neutrons with $E_n \approx 14.8$ MeV was measured with an NG-150 neutron generator. The T(d,n) reaction was used and the deuterons were accelerated to 130-140 keV. The procedure of measurement and processing of results was virtually identical to the conditions of measurement on the uranium assembly. The same ^{243}Am and ^{235}U layers were employed. During irradiation with the neutron generator the axis of each chamber with the fissile substance layer and the dielectric detector was arranged at an angle of about 55° to the neutron flux direction; in this geometry the influence of the angular anisotropy of the fragments is minimized. In these measurements the scattered neutron background did not exceed 2.6% for ^{243}Am and 4.0% for ^{235}U.

For $E_n \approx 14.8$ MeV the ^{235}U fission cross-section with allowance for impurity isotopes was taken as (2.223 ± 0.028) b per ^{235}U nucleus. As a result of the measurements, the following values were obtained: $\sigma_f{}^{243}\text{Am}/\sigma_f{}^{235}\text{U}$ ($E_n \approx 14.8$ MeV) = 1.023 ± 0.034; $\sigma_f{}^{243}\text{Am}$ ($E_n \approx 14.8$ MeV) = (2.275 ± 0.080) b. The total root-mean-square error has been given; the random error due to the statistical scatter of the number of tracks in the different series of measurement was 1.15%; the sources of systematic error have been listed above.

The ^{243}Am fission cross-section ($E_n \approx 14.8$ MeV) value obtained agrees satisfactorily with the results of Ref. [2] but lies somewhat below the value given in Ref. [5].

REFERENCES

[1] BUTLER, D.K., SJOBLOM, R.K., Phys. Rev. 124 (1961) 1129.

[2] FOMUSHKIN, Eh.F., GUTNIKOVA, E.K., ZAMYATIN, Yu.S. et al., Yad. Fiz. 5 (1967) 966.

[3] BOCA, I., MARTALOGU, N., SEZON, M. et al., Nucl. Phys. A. 134 (1969) 541.

[4] BRITT, H.C., WILHELMY, J.B., Nucl. Sci. and Engng. 72 (1979) 222.

[5] BEHRENS, J.W., BROWNE, J.C., ibid., 77 (1981) 444.

[6] LOZENZ, A., Proposed recommended list of transactinium isotopes decay date. Ph. 1: Half-lives. Dec. 1980, INDC(NDC)-121/NE.

[7] KON'SHIN, V.A., ZHARKOV, V.F., SUKHOVITSKIJ, E.Sh., Voprosy atomnoj nauki i tekhniki. Ser. Yadernye konstanty (Problems of Atomic Science and Technology, Ser. Nuclear Constants) 3(34) (1979) 3.

[8] NIKOLAEV, M.N., ibid. 6, Part 1 (1972) 10.

[9] FOMUSHKIN, Eh.F., GUTNIKOVA, E.K., NOVOSELOV, G.F., PANIN, V.I., At. Ehnerg. 39 (1975) 295.

[10] FOMUSHKIN, Eh.F., NOVOSELOV, G.F., VINOGRADOV, Yu.I. et al., Yad. Fiz. 33 (1981) 620.

[11] FOMUSHKIN, Eh.F., At. Ehnerg. 18 (1965) 178.

THE CROSS-SECTION OF THE $^{199}Hg(n,n')^{199}Hg^{m}$ REACTION FOR USE IN NEUTRON ACTIVATION MEASUREMENTS

(Original received 18 June 1984)

E.I. Grigor'ev and V.P. Yaryna

ABSTRACT

The paper gives the results of measurement and evaluation of the average reaction cross-section for the ^{235}U and ^{252}Cf fission spectra. The cross-section is evaluated in the 0.5-18 MeV region.

The $^{199}Hg(n,n')^{199}Hg^{m}$ reaction has advantages which favoured its use in the neutron activation measurements of reactor neutron field characteristics. The low reaction threshold (about 530 keV) and the convenient decay scheme of the reaction products are of importance. Since 1973 mercury detectors have been produced as part of the standardized set of neutron activation detectors of the AKN type [1], and although at that time full data were not available on the behaviour of the reaction cross-section, they were used successfully to determine the integral density of the fast neutron flux. In recent years there has been increased interest in this reaction and new data on its characteristics have appeared. The half-life of the $^{199}Hg^{m}$ nuclide is taken to be 42.6 $\pm$ 0.2 min, which is in agreement with the value of 42.8 min obtained by us; the emission of 158 keV gamma rays is (52.3 $\pm$ 0.5)% and of 374 keV gamma-rays (12.3 $\pm$ 0.5)% [2].

The data on the differential reaction cross-section have been supplemented by the results of the Japanese research group [3], which proposed not only experimental points in the 0.7-7 MeV region but also an analytical form of the cross-section dependence $\sigma(E)$ in a wide energy region. These data were taken as the basis of our evaluation of the cross-section behaviour. In addition, we used the form of cross-section behaviour in the 0.6-2.1 MeV region from Ref. [4] and the cross-section values for 14.1 and 14.4 MeV of 143 and 128 $\pm$ 20 mb, respectively [1].

Cross-section of the reaction $^{199}Hg(n,n')^{199}Hg^{m}$

E, MeV	σ, mb	E, MeV	σ, mb	E, MeV	σ, mb	E, MeV	σ, mb	E, MeV	σ, mb
5.00E-01	0.000E-00	5.25E-01	1.000E+00	5.50E-01	3.250E+00	5.75E-01	5.750E+00	6.00E-01	8.500E+00
6.30E-01	1.180E+01	6.60E-01	1.600E+01	6.90E-01	2.056E+01	7.20E-01	2.544E+01	7.60E-01	3.088E+01
8.00E-01	3.486E+01	8.40E-01	3.738E+01	8.80E-01	4.011E+01	9.20E-01	4.326E+01	9.60E-01	4.746E+01
1.00E+00	5.565E+01	1.10E+00	7.245E+01	1.20E+00	9.450E+01	1.30E+00	1.249E+02	1.40E+00	1.533E+02
1.50E+00	1.711E+02	1.60E+00	1.858E+02	1.70E+00	1.995E+02	1.80E+00	2.235E+02	1.90E+00	2.554E+02
2.00E+00	2.802E+02	2.10E+00	3.012E+02	2.20E+00	3.213E+02	2.30E+00	3.407E+02	2.40E+00	3.592E+02
2.50E+00	3.768E+02	2.60E+00	3.936E+02	2.70E+00	4.094E+02	2.80E+00	4.244E+02	2.90E+00	4.385E+02
3.00E+00	4.517E+02	3.10E+00	4.642E+02	3.20E+00	4.758E+02	3.30E+00	4.868E+02	3.40E+00	4.970E+02
3.50E+00	5.065E+02	3.60E+00	5.155E+02	3.70E+00	5.239E+02	3.80E+00	5.317E+02	3.90E+00	5.390E+02
4.00E+00	5.459E+02	4.10E+00	5.523E+02	4.20E+00	5.583E+02	4.30E+00	5.640E+02	4.40E+00	5.692E+02
4.50E+00	5.742E+02	4.60E+00	5.788E+02	4.70E+00	5.832E+02	4.80E+00	5.872E+02	4.90E+00	5.911E+02
5.00E+00	5.946E+02	5.10E+00	5.980E+02	5.20E+00	6.012E+02	5.30E+00	6.042E+02	5.40E+00	6.070E+02
5.50E+00	6.096E+02	5.60E+00	6.120E+02	5.70E+00	6.143E+02	5.80E+00	6.165E+02	5.90E+00	6.185E+02
6.00E+00	6.204E+02	6.10E+00	6.221E+02	6.20E+00	6.238E+02	6.30E+00	6.253E+02	6.40E+00	6.266E+02
6.50E+00	6.279E+02	6.60E+00	6.290E+02	6.70E+00	6.300E+02	6.80E+00	6.309E+02	6.90E+00	6.316E+02
7.00E+00	6.322E+02	7.10E+00	6.327E+02	7.20E+00	6.330E+02	7.30E+00	6.332E+02	7.40E+00	6.332E+02
7.50E+00	6.330E+02	7.60E+00	6.327E+02	7.70E+00	6.322E+02	7.80E+00	6.315E+02	7.90E+00	6.305E+02
8.00E+00	6.293E+02	8.10E+00	6.279E+02	8.20E+00	6.262E+02	8.30E+00	6.243E+02	8.40E+00	6.220E+02
8.50E+00	6.194E+02	8.60E+00	6.165E+02	8.70E+00	6.132E+02	8.80E+00	6.095E+02	8.90E+00	6.055E+02
9.00E+00	6.010E+02	9.10E+00	5.961E+02	9.20E+00	5.907E+02	9.30E+00	5.849E+02	9.40E+00	5.786E+02
9.50E+00	5.718E+02	9.60E+00	5.645E+02	9.70E+00	5.567E+02	9.80E+00	5.484E+02	9.90E+00	5.396E+02
1.00E+01	5.303E+02	1.01E+01	5.205E+02	1.02E+01	5.103E+02	1.03E+01	4.996E+02	1.04E+01	4.886E+02
1.05E+01	4.772E+02	1.06E+01	4.654E+02	1.07E+01	4.534E+02	1.08E+01	4.411E+02	1.09E+01	4.287E+02
1.10E+01	4.161E+02	1.11E+01	4.034E+02	1.12E+01	3.906E+02	1.13E+01	3.779E+02	1.14E+01	3.652E+02
1.15E+01	3.526E+02	1.16E+01	3.402E+02	1.17E+01	3.280E+02	1.18E+01	3.161E+02	1.19E+01	3.044E+02
1.20E+01	2.930E+02	1.21E+01	2.819E+02	1.22E+01	2.712E+02	1.23E+01	2.609E+02	1.24E+01	2.509E+02
1.25E+01	2.413E+02	1.26E+01	2.322E+02	1.27E+01	2.234E+02	1.28E+01	2.151E+02	1.29E+01	2.071E+02
1.30E+01	1.995E+02	1.31E+01	1.923E+02	1.32E+01	1.855E+02	1.33E+01	1.791E+02	1.34E+01	1.730E+02
1.35E+01	1.673E+02	1.36E+01	1.619E+02	1.37E+01	1.567E+02	1.38E+01	1.520E+02	1.39E+01	1.474E+02
1.40E+01	1.432E+02	1.41E+01	1.392E+02	1.42E+01	1.355E+02	1.43E+01	1.320E+02	1.44E+01	1.287E+02
1.45E+01	1.256E+02	1.46E+01	1.227E+02	1.47E+01	1.200E+02	1.48E+01	1.175E+02	1.49E+01	1.151E+02
1.50E+01	1.129E+02	1.51E+01	1.109E+02	1.52E+01	1.089E+02	1.53E+01	1.071E+02	1.54E+01	1.054E+02
1.55E+01	1.038E+02	1.56E+01	1.023E+02	1.57E+01	1.010E+02	1.58E+01	9.971E+01	1.59E+01	9.850E+01
1.60E+01	9.726E+01	1.61E+01	9.630E+01	1.62E+01	9.531E+01	1.63E+01	9.438E+01	1.64E+01	9.351E+01
1.65E+01	9.270E+01	1.66E+01	9.194E+01	1.67E+01	9.123E+01	1.68E+01	9.057E+01	1.69E+01	8.995E+01
1.70E+01	8.936E+01	1.71E+01	8.882E+01	1.72E+01	8.831E+01	1.73E+01	8.783E+01	1.74E+01	8.738E+01
1.75E+01	8.696E+01	1.76E+01	8.657E+01	1.77E+01	8.620E+01	1.78E+01	8.586E+01	1.79E+01	8.554E+01

The criterion of validity of the evaluated cross-section for integral experiments in reactor neutron fields was its consistency with the experimental values of the average reaction cross-section for the ^{235}U fission spectrum: 278 $\pm$ 23 mb [5], 252 $\pm$ 20 mb [6], 225 $\pm$ 10 mb [7], and with the average cross-section for the ^{252}Cf fission spectrum equal to 247 mb measured by us. The value in Ref. [5] was taken as the average of the results given and the value in Ref. [7] was adapted to the characteristics of the $^{199}Hg^{m}$ decay scheme given in this study. The value 225 $\pm$ 10 mb was taken as the recommended value since, in our opinion, the contribution of the associated reaction $^{198}Hg(n,\gamma)^{199}Hg^{m}$ may have been underestimated in Refs [5,6], while in Ref. [7] the mercury sample was irradiated in a boron shield eliminating the influence of the associated reaction, the influence of the shield being taken into account by means of a corresponding correction.

The evaluated cross-section is given in the Table in group form with the energy scale in the ENDF/B format. The value of the cross-section in each

energy group was obtained by linear interpolation between the boundaries of the group, and the obtained value was assigned to the lower boundary energy. The calculated value of the average cross-section for the ^{235}U fission spectrum using the present evaluation of the cross-section behaviour and the representation of the fission spectrum of the BKS-2 assembly [8] is 224 mb. For other descriptions of the fission spectrum, for example NBS and ENDF/B-V, the calculated cross-section differs insignificantly. For the ^{252}Cf fission spectrum in the representation of [9] the average cross-section is 241 mb.

In contrast to Ref. [1], the effective threshold and the reaction cross-section for a wide class of spectra were 1.4 MeV and 410 mb, respectively, with about 6% scatter of the cross-section values for different spectra.

REFERENCES

[1] VASIL'EV, R.D. GRIGOR'EV, E.I., NOZDRACHEV, S.Yu, YARYNA, V.P., in: The Metrology of Neutron Radiation in Reactors and Accelerators 1, Moscow, Izd. Standartov (1972) 194 (in Russian).

[2] SAKURAI, K., NUREG/CP-0029 (1982) 1, p. 373.

[3] SAKURAI, K. et al., J. Nucl. Sci. and Technology (1982) 19, N 10, p. 775.

[4] SWAN, C.P., METZGEN, F.R., Phys. Rev. (1955) 100, p. 1329.

[5] KOBAYASHI, K., KIMURA, I., INDC (JAP)-47/v, (Sept. 1979) p. 78.

[6] SAKURAI, K., KONDO, I., Nucl. Instrum. and Methods (1981) 187, p. 649.

[7] GRIGOR'EV, E.I., TARNOVSKIJ, G.B., YARYNA, V.P., "Measurement of the average cross-sections of threshold reactions for ^{235}U fission neutrons" in: Neutron Physics (Proceedings of the Sixth All-Union Conference on Neutron Physics) 3, TsNIIatominform, Moscow (1984) (in Russian).

[8] GRIGOR'EV, E.I., NOZDRACHEV, S.Yu., YARYNA, V.P., At. Ehnerg. 45, 3 (1978) 225.

[9] Nuclear data standards for nuclear measurements techn. rep. ser. N 227. Vienna: IAEA (1983).

EVALUATION OF THE ^{235}U FISSION CROSS SECTION IN THE 14.5-14.7 MeV NEUTRON ENERGY REGION

(Original received 9 February 1984)

V.N. Dushin, A.V. Fomichev, V.I. Shpakov
and S.S. Kovalenko

ABSTRACT

The ^{235}U fission cross-section in the neutron energy region of 14.5-14.7 MeV was evaluated on the basis of 12 experimental studies. The correlation matrix was obtained. The evaluated value of the fission cross-section (2.083 $\pm$ 0.015 b) was corrected by experts.

In order to generate the evaluated fission cross-section for $^{235}U(\sigma_{nf})$ in the 14.5-14.7 MeV neutron energy region, we considered the experimental studies [1-11] performed in nine laboratories in five different countries. For the correlation analysis we chose 11 experiments. We excluded Ref. [11] since this study was carried out with samples containing large (8%) amounts of other fissile substances and had a low accuracy (5-10%). The analysis consisted of several steps:

- Construction of the correlation matrix of the 11 experimental studies;
- Calculation of the average value and its dispersion;
- Correction of the result on the basis of expert evaluation.

The data contained in Refs [1-10] were used in constructing the correlation matrix. As we know [12], the fullest description of measurements guarantees the maximum objectivity in finding the correlation matrix. Where the description was not complete, the missing details were reconstructed by us on the basis of our understanding of the characteristics of the well-known procedures for fission cross-section measurement. In any experiment the final value measured σ_{nf} is a functional of the three generalized variables:

N_f, N_n, $n_{nucl.}$ ($\sigma_{nf} = N_f/N_n n_{nucl}$). The determination of each of the generalized variables is based on a procedure (method) with its set of elementary variables x_1, x_2, x_3, ... Some of these variables in different experiments performed by one method are independent (for example, counting statistics and geometrical factor), while others coincide fully (for example, tabular values of alpha-decay periods) or partly (for example, corrections calculated by one formula). Some variables (for example, fission-fragment anisotropy) may coincide when we go over from one procedure to another. An elementary error Δx_1, Δx_2, Δx_3, ... is associated with each variable. To establish the correlations, we used the following classification of the studies, depending on the measurement procedure:

- Those using an ionization chamber (all except Ref. [9]);
- Those using a track detector [9];
- Absolute measurements by the method of associated particles [1-4];
- Absolute measurements in relation to standards [9, 10];
- Measurements of the form with normalization in the low-energy part of the neutron spectrum [5-8];
- Alpha-count weighing in the geometry of small solid angles [1-4, 9, 10];
- Comparison with a standard sample in a thermal column [2];
- Direct weighing [4, 10].

N_f, N_n, n_{nucl} were represented as consisting of the following elementary variables:

In the case of use of an ionization chamber, $N_f = x_1 x_2 x_3 x_4$, where x_1 is the counting statistics minus background and random coincidences, x_2 the efficiency of the chamber as a function of fragment absorption in the layer, discrimination threshold and fission count losses due to "dead" time, x_3 the influence of the contribution of impurity isotopes and x_4 the inhomogeneity of the fissile substance layer.

In the case of use of a track detector, $N_f = x_5 x_6 x_7$, where x_5 is the fragment counting statistics, x_6 the geometrical factor and x_7 the correction for the angular distribution of fragments.

For absolute measurements by the method of associated particles, $N_n = x_8 x_9$, where x_8 is the statistics of associated particles minus background and x_9 the distortion of the neutron flux.

For absolute measurements in relation to standards, $N_n = x_{10} x_{11}$, where x_{10} is a variable associated with the measurement procedure and x_{11} a variable associated with normalization in relation to the standard.

For measurements of the form with normalization in the low-energy region of the neutron spectrum, $N_n = (x_{12} - x_{13}) x_{14} x_{15}$, where x_{12} is the flux monitor count, x_{13} the flux monitor background, x_{14} the correction for neutron absorption and x_{15} the normalization factor.

For alpha-count weighing in the geometry of small solid angles, $n_{nucl} = x_{16} x_{17} x_{18}$, where x_{16} is the alpha counting statistics minus backgrounds, x_{17} the geometrical factor and x_{18} the alpha decay period.

For comparison with a standard sample in the thermal column $n_{nucl} = x_{19} x_{20}$, where x_{19} is the error of the standard and x_{20} the correction for neutron scattering and absorption.

For direct weighing, $n_{nucl} = x_{21}$, where x_{21} is the result of direct weighing.

In constructing the correlation matrix one of three levels of correlation between the elementary components of error was taken: zero ($K = 0$), full correlation ($K = 1$) and intermediate level ($K = 0.7$). As a result, we obtained the matrix for finding the preliminary weights with which the results of the individual experiments were considered. The formal procedure of construction of the correlation matrix [12] does not cover the whole of the available information on the situation during measurement of the fission cross-section. Therefore, in addition to the statistical analysis, an

Table

Covariant matrix of the results of the ^{235}U fission cross-section measurements

Ref.	σ_{nf}	I	2	3	4	5	6	7	8	9	IO	II
[I] *	2,095	2,5	0,682	0,629	0,904	0,904	0,02	0,02I	0,033	0,033	0,22I	0,69I
[I] **	2,079		2,06	0,575	0,770	0,904	0,02	0,0I5	0	0	0,220	0,69I
[2]	2,080			2,25	0,904	0,904	0,02I	0,02I	0,033	0,033	0,22I	0,75I
[3]	2,063				4	I,552	0,033	0,043	0,033	0,033	0,49	I,33I
[4]	2,098					4	0,02	0,02	0,033	0,033	0,49	0,44I
[5]	2,075						5	I	I8,2	I8,2	0	0,02
[6]	2,06							9	I8,2	I8,2	0	0,02
[7]	2,I86								26	25	0	0
[8]	2,I8									26	0	0
[9]	2,070										4,84	0,35
[IO]	2,22											6,25

[*] Result of six measurements made at the V.G. Khlopin Radium Institute, USSR.

[**] Result of five measurements made at the Technical University, Dresden, German Democratic Republic.

expert evaluation was made of particular experiments. The following factors were taken into account:

1. The experiments in Ref. [1-4] were made by one method - that of time-correlated associated particles. The measurements in Ref. [3] were performed independently of Ref. [1], whose authors worked in close collaboration. The work in Ref. [2] was carried out when the results of Refs [1, 3] had already been published. The experimental set-up in Ref. [4] was evidently a repetition of one of the earlier variants of that of the V.G. Khlopin Radium Institute;
2. The form with normalization in the low-energy part of the neutron spectrum was measured in Refs [5-8]. In Ref. [6] the measurements were made by the procedure and with the set-up developed in Ref. [5]. However, in these measurements a different form of the $\sigma_{nf}(E_n)$ curves was obtained. The studies in Refs [7-8] were carried out with the same set-up although the forms of the curves

obtained were different. All this indicates the presence of hidden systematic errors in the procedure of measurement of the form.

Changes corresponding to the above comments were made in the matrix obtained on the basis of the formal correlation analysis. The final form of the matrix is shown in the table. The fission cross-section obtained from 11 experiments and calculated with the help of the correlation matrix on the basis of the data in the table is proposed as an evaluated value equal to 2.083 ± 0.015 b.

REFERENCES

[1] DUSHIN, V.N., FOMICHEV, A.V., KOVALENKO, S.S., et al. At. Ehnerg. 55, 4 (1983) 218-222.

[2] WASSON, O.A., CARLSON, A.D., DUVALL, K.C., Nucl.Sci. and Engng, 80, (1982) 282.

[3] CANCE, M., GRENIER, G. Ibid. 68, (1978), 197.

[4] LI JINGWEN, LI ANLI, RONG CHAOFAN, et al., in: Proc.Intern. Conf. on "Nucl.Data for Science and Technology". Belgium, Antwerpen, 1982.

[5] CZIRR, J.B., SIDHU, G.S., Nucl. Sci. and Engng, 57, (1975), 18.

[6] LEUGERS, B., CIERJACKS, S., BROTZ, P., et al., in: Proc. NEANDC/NEACRP. Specialists' Meeting ANL-76-90, 246.

[7] CARLSON, A.D., PATRICK, B., in: Proc. of 2nd Conf on Neutron Cross-section and Technology. Harwell, (1978) 880.

[8] KARI, K., KFK-2673, (1978).

[9] MAHDAVI, M., KNOLL, G.F., in: [5], 58.

[10] WHITE, P.H., J.Nucl.Energy, 19, (1965), A/B, 325.

[11] PANKRATOV, V.M., At. Ehnerg. 14, (1963) 177.

[12] MANNHART, W., PTB-FMRB-84. Braunshweig, (1981).

ANALYTICAL REPRESENTATION ON THE BASIS OF THE PADE APPROXIMATION OF THE THRESHOLD REACTION CROSS-SECTIONS FROM THE DOSIMETRY FILE

(Original received 25 January 1984)

S.A. Badikov, A.I. Blokhin, E.V. Gaj, V.N. Manokhin and N.S. Rabotnov

ABSTRACT

Approximation by rational functions has been used to convert into the analytical form the evaluated data on the neutron-induced threshold reaction cross-sections from the International Reactor Dosimetry File. In some cases, a comparison was made with the results of similar processing of the BOSPOR library data.

The method developed in the recent years for processing data on the basis of the Pade approximation by rational functions [1] offers a convenient way of representing in the analytical form the energy dependences of neutron cross-sections, both experimental and evaluated. In particular, the threshold reactions data collected in the BOSPOR library [2, 3] were converted into this representation. This not only enables us to calculate rapidly the cross-section value for any energy $E_n \leq 20$ MeV but also to reduce the volume of numerical information to be stored by more than an order in comparison with the point representation.

The efficiency of the above method of approximation depends appreciably on the nature of the material processed, especially on the analytical nature of the functional dependence represented in the form of a discrete set of $\sigma(E_i)$ values. In processing experimental data we can consider that:

$$\sigma(E_i) = \tilde{\sigma}(E_i) + \delta(E_i), \qquad (1)$$

where $\tilde{\sigma}(E_i)$ is an analytical function and $w(E_i)$ a small random addition whose statistical distribution is approximately known and is usually assumed to be normal. For such a situation a method was developed for evaluation of

the errors of the approximant [4] and considerable experience has been accumulated on its practical use.

Although evaluated data are also represented in the form of $\sigma(E_i)$, they often have a different character in that the dependence $\sigma(E)$ is already the result either of some approximation of experimental data or of calculations using a specific theoretical model, i.e. $\sigma(E)$ is a piecewise smooth function, and the number of intervals with a different dependence can be quite large.

Such is precisely the character of neutron data represented in the widely used format of the ENDF/B library [5]. These are piecewise smooth functions obtained by reducing the approximating dependences of five types: linear-linear, linear-logarithmic, etc., so that there are difficulties in approximating them by a single analytical expression. Moreover, from the standpoint of rational approximation many cross-sections in the ENDF/B library, especially the threshold reaction cross-sections, have an inconvenient characteristic in that a very large drop in values occurs when one goes into the sub-barrier region - by as much as 15-20 orders in some cases. These values are not reliable since in many cases they are not based on measurement results; moreover, because of their smallness they play no part in neutron physics calculations. However, in the approximation by rational functions it is these small values that create one of the main difficulties: rational approximants contain neither factor nor exponential small values; they can be obtained in the approximants only as a difference of values of one order with an understandable loss of accuracy.

For these reasons, from the standpoint of verification of the Pade approximation method there was interest in trial processing the data in the ENDF/B format. For such processing the neutron-induced threshold reaction cross-sections from the International Reactor Dosimetry File [6] were chosen as the first example. We also intended to compare the processing results with

Table 1

Reactions	Table No.	Reactions	Table No.
$^{6}Li(n,^{4}He)$ (left-hand part)	6	$^{54}Fe(n,p)^{54}Mn$	2
$^{6}Li(n,^{4}He)$ (right-hand part)	6	$^{55}Mn(n,2n)^{54}Mn$	8
$^{10}B(n,^{4}He)$ (left-hand part)	6	$^{56}Fe(n,p)^{56}Mn$	5
$^{10}B(n,^{4}He)$ (right-hand part)	2	$^{58}Ni(n,p)^{58}Co$	3
$^{27}Al(n,p)^{27}Mg$ (left-hand part)	8	$^{58}Ni(n,2n)^{57}Ni$	8
$^{27}Al(n,p)^{27}Mg$ (right-hand part)	3	$^{59}Co(n,2n)^{58}Co$	8
$^{27}Al(n,\alpha)^{24}Na$	5	$^{59}Co(n,\alpha)^{56}Mn$	7
$^{32}S(n,p)^{32}P$	2	$^{60}Ni(n,p)^{60}Co$	2
$^{46}Ti(n,p)^{46}Sc$	5	$^{63}Cu(n,\alpha)^{60}Co$	3
$^{47}Ti(n,p)^{47}Sc$	3	$^{65}Cu(n,2n)^{64}Cu$	8
$^{47}Ti(n,n'p)^{46}Sc$	7	$^{115}In(n,n')$ (left-hand part)	4
$^{49}Ti(n,p)^{49}Sc$	4	$^{115}In(n,n')$ (right-hand part)	4
$^{49}Ti(n,n'p)^{48}Sc$	7	$^{127}I(n,2n)^{126}I$	7

the analytical representation of the BOSPOR library [3] in the case of reactions whose cross-sections are represented in both libraries.

The Pade approximation of the second kind, used for the processing, represents the energy dependence of the cross-section in the form of the rational function $f^{[L]}(E) = P_N(E)/Q_M(E)$, where P_N and Q_M are polynomials of degrees N and M, respectively and $L = N + M + 1$ is the total number of parameters of the approximant. The most convenient for neutron-physics applications is the representation of $f^{[L]}(E)$ in the form of a pole expansion (for $N \leq M$):

$$f^{[L]}(E) = C + \sum_{i=1}^{\ell_1} \frac{a_i}{E-p_i} + \sum_{k=1}^{\ell_2} \frac{\alpha_k(E-\varepsilon_k)+\beta_k}{\gamma_k^2+(E-\varepsilon_k)^2}, \qquad (2)$$

where the real poles P_i should lie outside the interval considered.

The International Reactor Dosimetry File [6] includes data on the cross-section of 22 threshold reactions. As a result of our processing all of

them were represented by expressions of type (2), and the resulting sets of parameters are given in Tables 1-8 [*]. In four cases, the approximation interval was divided into two parts. Because of the above-mentioned difficulty of describing small values of cross-sections all values differing from the maximum by a factor of more than 10^6 were assumed to be zero and the approximation interval was reduced accordingly.

The description of the set of points of the file had an average relative accuracy higher than 3% in most cases (18 curves); the corresponding figures are given in Tables 2-8. The complex curve of the reaction $^{32}S(n,p)^{32}P$ had the lowest index of relative accuracy (7%). It is shown in Fig. 1. It should be noted that the data for precisely this cross-section represented the only case out of 140 curves of the BOSPOR library for which in Ref. [3] no satisfactory result of approximation could be obtained because of the large number of irregularities.

Table 2

Parameter	Reaction			
	$^{10}B(n,^4He)$ (right-hand part)	$^{54}Fe(n,p)^{54}Mn$	$^{60}Ni(n,p)^{60}Co$	$^{32}S(n,p)^{32}P$
α_1	2,4I542 + I	-5,93095 - I	2,6708I - I	7,49552 - 2
β_1	-I,87296 + 2	I,53890 + I	2,I2694 0	5,67687 0
ε_1	-3,22756 - 0	I,09842 + I	I,00295 + I	I,05538 + I
γ_1	I,00757 + I	6,I7392 0	3,66946 0	3,84387 0
α_2	6,7I850 - I	6,09475 - I	3,58869 - 2	4,II467 - 2
β_2	-3,79442 - 2	-8,40358 - 2	-9,67I26 - 2	I,II569 - I
ε_2	-9,62483 - 2	3,54848 0	5,68053 0	3,7I097 0
γ_2	I,4I3I9 - I	2,05I84 0	2,I3304 0	5,47824 - I
α_3	-3,83745 - I	2,08757 - 3	3,79095 - 3	I,I4333 - I
β_3	8,4I748 - I	7,58980 - 3	-7,I7559 - 3	I,II507 - I
ε_3	5,49434 - 0	3,06658 0	I,I0I27 + I	5,78448 0
γ_3	I,59755 - 0	3,23752 - I	3,09036 - I	9,89I06 - I
α_4	-7,83680 - 3	I,92778 - 3	6,22424 - 4	5,I2899 - 2
β_4	6,68403 - 2	-I,36040 - 4	-6,68267 - 4	-9,05343 - 3
ε_4	I,88652 0	I,9I35I 0	4,30249 0	3,9I524 0
γ_4	3,59463 - I	I,93256 - I	5,79434 - I	I,98874 - I
α_5	-8,I6269 - 3	4,7I322 - 7	-9,82087 - 6	I,42668 - 2
β_5	I,84690 - 2	5,0I907 - 8	9,07036 - 6	3,64704 - 3
ε_5	2,80089 0	I,00490 0	4,I2557 0	2,28039 0
γ_5	3.I60I0 - I	-3,6008 - 2	I,92I89 - I	2,69258 - I

[*] Table 1 can be used to search for the necessary reaction.

Table 2 (continued)

Parameter	Reaction			
	$^{10}B(n,^4He)$(right-hand part)	$^{54}Fe(n,p)^{54}Mn$	$^{60}Ni(n,p)^{60}Co$	$^{32}S(n,p)^{32}P$
α_6	-4,52613 - 3	-	-I,47592 - 6	2,47819 - 3
β_6	2,32146 - 3	-	I,27568 - 7	2,26354 - 5
ε_6	5,15128 - I	-	4,02196 0	2,7487I 0
γ_6	I,II55I - I	-	5,66130 - 2	5,54519 - 2
α_1	I,I3264 - I	-6,00054 - 5	-	-
β_1	-2,I9145 - 2	6,02300 - I	-	-
α_2	2,24315 - 2	-	-	-
β_2	-6,24I4I - 4	-	-	-
C	0,0	0,0	I,37680 - 2	0,0
L	28	22	25	24
SUM,%	2,03	2,58	3,3	7,0
S,%	-	II,9	43,7	-
GR, eV	$I0^3$	$83,4 \cdot I0^4$	$3,54 \cdot I0^6$	$I0^6$

Table 3

Parameter	Reaction			
	$^{27}Al(n,p)^{27}Mg$ (right-hand part)	$^{58}Ni(n,p)^{58}Co$	$^{63}Cu(n,\alpha)^{60}Co$	$^{47}Ti(n,p)^{47}Sc$
α_1	3,62135 - I	2,60163 0	-4,47295 - 2	3,98716 - I
β_1	2,08663 0	I,I0398 + I	3,I6336 - I	5,35194 0
ε_1	8,I5974 0	4,52809 0	1,II433 + I	9,57974 0
γ_1	4,80659 0	5,I0225 0	2,44066 0	6,70652 0
α_2	I,76193 - 3	-5,77524 - I	6,60810 - 2	I,I0000 - I
β_2	-2,99232 - 3	I,60167 0	I,96349 - I	4,86689 - 2
ε_2	4,24895 0	I,35355 I	I,36595 + I	2,89129 0
γ_2	5,23988 - I	3,I9457 0	2,73696 0	2,II697 0
α_3	-I,23127 - 3	-I,78570 - I	9,70796 - 3	-I,96596 - 3
β_3	-4,70III - 5	-4,50738 - I	-3,89852 - 2	3,77225 - 5
ε_3	4,74479 0	I,44534 0	5,74129 0	2,56072 0
γ_3	I,23935 - I	I,8925I 0	2,5I067 0	I,7I659 - I
α_4	2,87610 - 4	-I,09434 - 4	2,30467 - 3	-3,23189 - 4
β_4	4,I2347 - 5	-2,57504 - 3	-8,38305 - 4	I,74212 - 5
ε_4	3,47511 0	2,09945 0	8,22650 0	I,34038 0
γ_4	7,57711 - 2	3,87797 - I	5,54922 - I	I,I7329 0
α_5	2,36399 - 4	4,67I84 - 5	-3,20727 - 8	-8,23657 - 5
β_5	-3,8564I - 6	2,72264 - 6	I,74348 - 8	-8,75808 - 6
ε_5	3,62267 0	9,94734 - I	3,04010 0	I,58537 0
γ_5	4,2I889 - 2	I,07085 - I	I,29229 - I	8,03738 - 2
C	0,0	0,0	0,0	0,0
L	20	20	20	20
SUM,%	3,97	I,08	I,58	2,44
S,%	-	I5	-	8,73
GR, eV	$3,0I \cdot I0^6$	$0,6I2 \cdot I0^6$	$2,5 \cdot I0^6$	$I,I5 \cdot I0^6$

Table 4

Parameter	Reaction		
	$^{115}In(n,n')$ (left-hand part)	$^{115}In(n,n')$ (right-hand part)	$^{49}Ti(n,p)^{49}Sc$
α_1	I,57448 - 5	I,0I687 - 0	2,0I36I - I
β_1	-I,I0969 - 4	2,I3868 - I	I,3358I - 0
ε_1	5,7I475 - I	4,348I2 - 0	I,25090 + I
γ_1	I,24622 - I	2,9I42I - 0	4,89098 - 0
α_2	I,44395 - 7	2,45I92 - I	3,50343 - 3
β_2	-7,60292 - 9	I,39382 - 0	I,02693 - 3
ε_2	3,5425I - I	2,34528 - 0	7,I6644 - 0
γ_2	5,7I2I4 - 3	I,7796I - 0	I,33684 - 0
α_3	4,66527 - 7	-2,223I9 - I	2,64278 - 5
β_3	-I,04086 - 9	-9,82683 - 2	-3,III73 - 5
ε_3	3,49I65 - I	I,2I432 + I	5,7I495 - 0
γ_3	4,II762 - 3	2,I3246 - 0	2,I0I92 - I
α_4	-	5,I769I - 4	-2,2I337 - 6
β_4	-	-6,6838I - 5	-7,3I478 - 6
ε_4	-	I,II038 - 0	5,I2324 - 0
γ_4	-	6,05449 - 2	I,992I5 - I
α_1	-I,33722 - 2	-	I,I5484 - 2
ρ_1	-5,96787 - I	-	I,7I0I2 - 0
α_2	-I,24940 - 2	-	-
ρ_2	I,I2I74 - 0	-	-
C	0,0	0,0	0,0
L	I6	I6	I8
SUM,%	2,25	2,58	2,65
S,%	-	-	97
GR,eV	$0,34 \cdot I0^6$	$0,90 \cdot I0^6$	$4,4 \cdot I0^6$

Table 5

Parameter	Reaction		
	$^{56}Fe(n,p)^{56}Mn$	$^{27}Al(n,\alpha)^{24}Na$	$^{46}Ti(n,p)^{46}Sc$
α_1	I,30567 - I	-I,7II5I - I	2,4I952 - I
β_1	2,06932 - 0	2,40704 - 0	I,50620 + I
ε_1	I,25997 + I	I,43I29 + I	I,204I0 + I
γ_1	4,39738 - 0	4,856I9 - 0	7,90379 - 0
α_2	2,II728 - 2	I,72906 - I	2,82482 - I
β_2	-I,57990 - 2	-9,29483 - 2	-3,89585 - I
ε_2	5,885I3 - 0	8,06589 - 0	5,07422 - 0
γ_2	I,36857 - 0	3,03892 - 0	2,84986 - 0
α_3	3,08635 - 6	-8,7650I - 4	9,93I59 - 3
β_3	5,49I00 - 9	-8,76II8 - 3	-4,6648I - 3
ε_3	4,56402 - 0	6,20I95 - 0	3,72099 - 0
γ_3	I,50260 - I	I,I320I - 0	8,3I888 - I
α_1	-2,I6I05 - 3	-	-
ρ_1	2,03363 + I	-	-
0	0,0	0,0	0,0
L	I4	I2	I2
SUM,%	I,38	0,694	0,697
S,%	8,27	5,7	I8,3
GR, eV	$4,085 \cdot I0^6$	$3,6 \cdot I0^6$	$2,75 \cdot I0^6$

Table 6

Parameter	Reaction			Parameter	Reaction		
	$^{6}Li(n,^{4}He)$ (right-hand part)	$^{6}Li(n,^{4}He)$ (left-hand part)	$^{10}B(n,^{4}He)$ (left-hand part)		$^{6}Li(n,^{4}He)$ (right-hand part)	$^{6}Li(n,^{4}He)$ (left-hand part)	$^{10}B(n,^{4}He)$ (left-hand part)
a_1	3,47966 + I	2,80663 - 4	3,2632I - 2	α_1	9,28460 - I	-	-
p_1	-7,60755 + I	-I,6I484 - 6	-I,34I83 - 3	β_1	I,67399 - I	-	-
a_2	I,79876 - 2	3,25260 - 5	3,88602 - 3	ε_1	3,26572 0	-	-
p_2	-I,2II56 - 2	-5,57096 - 8	-4,26003 - 5	γ_1	I,52468 0	-	-
a_3	3,I7443 - 3	7,59983 - 6	8,38272 - 4	α_2	8,98463 - 3	-	-
p_3	-4,73672 - 4	-3,24II5 - 9	-2,06834 - 6	β_2	5,97580 - 3	-	-
a_4	6,80464 - 4	I,89529 - 6	I,86393 - 4	ε_2	2,39750 - I	-	-
p_4	-2,30298 - 5	-I,89389 - I0	-I,06825 - 7	γ_2	4,46593 - 2	-	-
a_5	I,93II7 - 4	5,64333 - 7	4,30393 - 5	C	0,0	0,0	0,0
p_5	-7,59328 - 7	-6,50484 - I2	-5,76676 - 9	L	I8	I0	I4
a_6	-	-	I,02088 - 5	SUM,%	2,37	0,28I	0,433
p_6	-	-	-2,94899 - I0	S,%	-	-	-
a_7	-	-	2,76345 - 6	GR,eV	$I,03\cdot I0^{6}$	$I0^{-5}$	$I0^{-5}$
p_7	-	-	-8,90857 - I2				

Table 7

Parameter	Reaction			
	$^{59}Co(n,\alpha)^{56}Mn$	$^{47}Ti(n,n'p)^{46}Sc$	$^{49}Ti(n,n'p)^{48}Sc$	$^{127}I(n,2n)^{126}I$
α_1	I,95227 - 2	I,36264 - I	7,3734I - 2	4,25864 - 0
β_1	4,I64I7 - I	3,34730 0	5,88756 - I	2,95662 0
ε_1	I,38640 + I	I,78I89 + I	I,8I649 + I	I,082I2 + I
γ_1	3,93049 0	4,8I493 0	3,46422 0	3,06684 0
α_2	I,54067 - 2	9,7399I - 2	-2,0II30 - 4	-I,92I82 0
β_2	8,7I290 - 3	-I,49527 - I	-7,04837 - 3	7,96I95 0
ε_2	8,02446 0	I,385I7 + I	I,39450 + I	I,72833 + I
γ_2	2,32354 0	2,I7638 0	I,4II89 0	2,85804 0
C	0,0	0	0	0
L	8	8	8	8
SUM,%	2,6I	0,77	I,I4	0,82
S,%	2,5	-	-	27,2
GR, eV	$5,5\cdot I0^{6}$	$I0,6\cdot I0^{6}$	$II,6\cdot I0^{6}$	$9,23\cdot I0^{6}$

In the case of 14 curves which were also processed on the basis of the BOSPOR data, the resulting curves were compared by calculating the average relative deviation:

$$S = \sqrt{\frac{1}{N}\sum_{i=1}^{N}\frac{(F_{1i}-F_{2i})^2}{F_{1i}^2}}\ , \qquad (3)$$

where F_{1i}, F_{2i} are the values of the approximant obtained from the data of the BOSPOR library and the Reactor Dosimetry File, respectively, at the i-th

Table 8

Parameter	Reaction				
	$^{27}Al(n,p)^{27}Mg$ (left-hand part)	$^{55}Mn(n,2n)^{54}Mn$	$^{59}Co(n,2n)^{58}Co$	$^{58}Ni(n,2n)^{57}Ni$	$^{65}Cu(n,2n)^{64}Cu$
α_1	2,98522 - 4	2,28630 0	4,73786 - I	-I,22684 - I	-I,99659 0
β_1	-I,I643I - 4	-6,95427 0	I,04572 - I	2,7536I - 2	-3,I4980 0
ε_1	2,85I05 0	I,09902 + I	I,30266 + I	I,I8357 + I	9,59396 0
γ_1	4,857I0 - I	3,2II60 0	I,82I36 0	5,5I78I - I	I,67869 0
a_1	-5,43075 - 4	3,97733 - 3	-5,29853 0	-	9,84587 - 2
p_1	3,33723 0	I,05804 + I	6,70779 0	-	2,04639 + I
a_2	-	-	I,55785 0	-	-
p_2	-	-	2,44I85 + I	-	-
C	0	7,20446 - I	I,48579 0	7,2 - 2	I,407 - 0
L	6	7	9	5	7
SUM,%	0,3I8	I,46	0,38	I,77	0,58
S,%	-	I3,0	I0,0	I3,6	8,74
GR,eV	$2,4I \cdot I0^6$	$I0,4 \cdot I0^6$	$I0,6 \cdot I0^6$	$I2,4 \cdot I0^6$	$I0,06 \cdot I0^6$

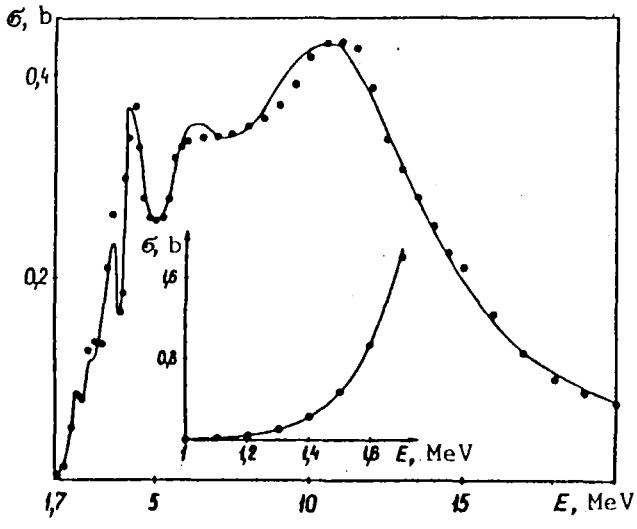

Figure 1. Results of processing the $^{32}S(n,p)^{32}P$ reaction cross-section data from the file [6]: the points indicate initial data and the continuous curves the Pade approximant.

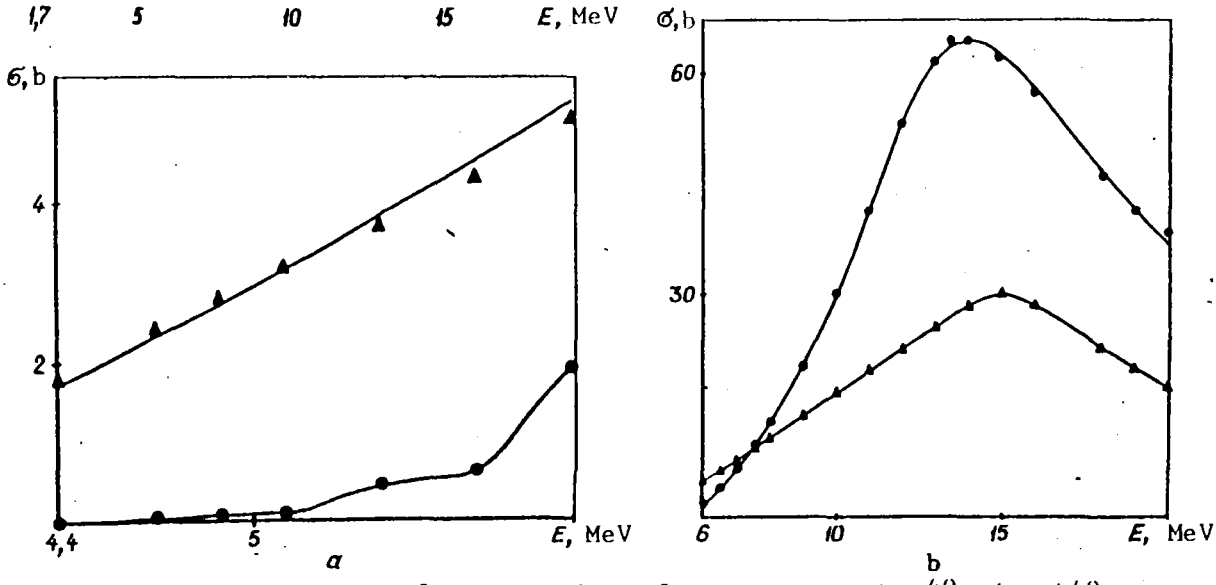

Figure 2. Comparison of the results of processing the $^{49}Ti(n,p)^{49}Sc$ reaction cross-section data in the 4.4-6 MeV region (a) and in the 6-20 MeV region (b) in two variants: ● - Reactor Dosimetry File data; ▲ - BOSPOR library data; the curves represent the results of the Pade approximation [6].

point. These values are also given in Tables 2-8. In Fig. 2 we consider the case of the greatest difference between the BOSPOR and ENDF evaluations: the cross-section of the reaction $^{49}Ti(n,p)^{49}Sc$ when S = 97%.

In Tables 2-8, for each reaction we have also given the attained relative accuracy of description in % (parameter SUM) and the lower boundary of the energy range GR, over which the approximation was performed.

REFERENCES

[1] Vinogradov, V.N., Gaj, E.V., Rabotnov, N.S., The Use of the Pade Approximation of the Second Kind in the Resonance Analysis of Neutron Cross-sections. Report FEhI-484. Obninsk (1975) (in Russian); The Method of Reference Ordinates in the Processing and Analysis of Experimental Dependences. Report FEhI-1328. Obninsk (1982) (in Russian).

[2] Bychkov, V.M., Manokhin, V.N., Pashchenko, A.B., Plyaskin, V.I., "The cross-sections of the threshold reactions (n,p), (n,α), (n,2n). Parts I, II" in: Problems of Atomic Science and Technology. Series Nuclear Constants 1 (32) (1979) 27 (in Russian).

[3] Badikov, S.A., Vinogradov, V.N., Gaj, E.V., et al. "Analytical representation on the basis of the Pade approximation of evaluated data on neutron-induced threshold reaction cross-sections", ibid. 3 (47) (1982) 66 (in Russian).

[4] Badikov, S.A., Gaj, E.V., Rabotnov, N.S., "Determination of errors of resonance curves on the basis of the Pade approximation", ibid. 3 (52) (1983) 11 (in Russian).

[5] Data formats and procedures (ENDF-102). Revised by R. Kinsey (1979) BNL-NCS-50496.

[6] The international reactor dosimetry file (IRDF-82). Assembled by D.E. Cullen, N. Kocherov, P.M. McLaughlin (1982) IABA-NDS-41.